IOP Publishing Journal of Physics B: Atomic, Molecular and Optical Physics

J. Phys. B: At. Mol. Opt. Phys. **40** (2007) 3851–3860 doi:10.1088/0953-4075/40/19/006

Coherent population trapping in a finite-size buffer-less cell

Georgy Kazakov[1], Boris Matisov[1], Andrey Litvinov[2] and Igor Mazets[3]

[1] Theoretical Physics Department, St Petersburg State Polytechnical University, Polytechnicheskaya 29, St Petersburg 195251, Russia
[2] Solid State Physics Department, A F Ioffe Physico-Technical Institute, Polytechnicheskaya 26, St Petersburg 194021, Russia
[3] Plasma Physics Department, A F Ioffe Physico-Technical Institute, Polytechnicheskaya 26, St Petersburg 194021, Russia

E-mail: kazjor@rambler.ru, anprolvy@list.ru and mazets@astro.ioffe.rssi.ru

Received 13 July 2007, in final form 24 August 2007
Published 19 September 2007
Online at stacks.iop.org/JPhysB/40/3851

Abstract

We have investigated theoretically the formation of a coherent population trapping resonance in a finite-size vapour cell without a buffer gas. We have demonstrated the novel mechanisms of the resonance narrowing: an analogue of the Dicke effect and light-induced narrowing. In the light-induced narrowing regime the parameters of the coherent population trapping resonance weakly depend on the cell size and the type of coating.

1. Introduction

Coherent population trapping (CPT) in atomic vapours and the related effect of electromagnetically-induced transparency (EIT) in coherent media are subjects of continuous interest for many research groups. This interest, besides the fundamental aspects of these phenomena, is caused by various possible applications of the CPT and EIT effects, such as trapping of ions [1], slowing down and storage of light [2, 3], quantum information storage and processing [4], development of the new types of frequency standards (atomic clocks) (see [5–7]) and magnetometers (see [8, 9]), high-resolution spectroscopy (see [10, 11]) and subrecoil laser cooling of atoms [12].

The physical essence of CPT is the accumulation of the whole population in a certain quantum superposition state of a multilevel quantum system, which is decoupled from the incident laser radiation consisting of a few mutually correlated modes [13]. CPT exists in a narrow range of the difference of the frequencies of the involved laser modes, near a two-photon resonance. By scanning one frequency, while the others are kept fixed, one can observe a narrow (much narrower than the natural line width of the optically excited state) resonant dip in the absorption spectrum. Such a sharp frequency dependence allows for various

applications of CPT. EIT is, in fact, CPT in an optically dense medium, or in a pulse regime of laser radiation, or in the case when one laser component (drive) is much stronger than the other (probe).

Quantum frequency standards (atomic clocks) are widely used in many scientific and technological applications, such as positioning and navigation systems, telecommunication networks, high-precision set-ups for testing the fundamental laws of physics, etc. Vapour-cell-based standards are now at the frontiers of development of the secondary standards, because of the rapid progress in the relevant laser techniques. CPT-based quantum frequency standards (see [14]) comprise a specific class of atomic clocks, since their set-ups do not include microwave cavities (in contrast to the formerly used atomic clocks based on a double radio-optical resonance). The absence of a cavity is a key factor in miniaturization of frequency standards. CPT-based atomic clocks with dimensions of about a few millimetres have been developed (see [6]).

The figure-of-merit is one of the most important parameters of a quantum discriminator. It is determined by a few CPT parameters, such as amplitude, width and contrast. In particular, the shorter the mean time of coherent interaction between an atom and the resonant laser field, the lower the figure-of-merit. In other words, relaxation of the coherence between the atomic states comprising the working transition due to atom–atom and atom–wall collisions imposes major limitations to the figure-of-merit value (see [15] for more details).

Several methods of increasing the atom–field coherent interaction time are known. For example, a buffer gas can be admixed to the active medium in a cell. Usually, inert gases, methane or nitrogen are used as a buffer gas. Active atoms collide with the buffer gas atoms or molecules. Therefore, their mean free paths increase significantly, leading to efficient suppression of relaxation due to the wall collisions. This effect was first discovered by Dicke in [16]. The presence of a buffer gas can reduce the CPT resonance width to values as low as 40 Hz (see [17]).

On the other hand, the presence of a buffer gas negatively affects the CPT resonance, in particular shifts and broadens the working transition, mixes Zeeman sublevels, etc. To circumvent this difficulty, one may use a method proposed by Robinson and co-workers nearly 50 years ago [18]. This method implies coating of the cell walls with an anti-relaxation material (most commonly, paraffin). Anti-relaxation coating significantly (by four orders of magnitude [19]) decreases the atomic coherence relaxation rate due to atom–wall collisions. In other words, the atomic superposition state corresponding to CPT survives a collision with a wall with probability very close to 1. As a result, the time of coherent interaction of an atom with the resonance multimode laser light increases by the same four orders of magnitude. The narrowing of the double radio-optical resonance line was detected experimentally in [18, 20], and the corresponding theory was developed in [21, 22]. Recent progress in laser techniques has given a new momentum to the experimental studies of coherent excitation of atomic vapours in coated cells (see [23, 24]). In particular, cells with a coating made more than 40 years ago have been tested in [23]. The results demonstrate quite weak degradation of the anti-relaxation coating due to the 'ageing': the estimation of the working transition line shift is less than 10 Hz per 30 years.

Recalling the analogy with the double radio-optical resonance, one may expect that the CPT resonances in coated cells are quite narrow. Indeed, there are many observations of narrow EIT resonances [4, 25, 26]. However, the CPT line narrowing has been observed not only for coated cells, but for cells without coating (vacuum cells) as well [25, 26]. This narrowing has been observed for cell lengths a larger than the range of relaxation suppression $qa \ll 1$, according to the Dicke theory. In fact, the product qa in some cases was of the order of 1 and sometimes even appreciably exceeded 1. $\vec{q} = \vec{k}_1 - \vec{k}_2$, $\vec{k}_1$ and $\vec{k}_2$

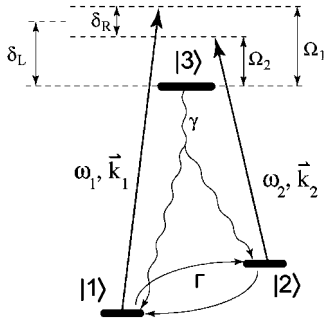

Figure 1. Λ-system excitation scheme.

are the wave vectors of a two-mode laser field (see figure 1). These results are explained within the theory of laser-induced line narrowing (LILN), which was first developed in [27]. This effect has been investigated theoretically in many works [28–30]; however, the effects of the finite size of the cell have been neglected.

Therefore, investigation of CPT and EIT in finite-size cells is a timely problem and can have a wide variety of promising practical applications. In the present work, we investigate theoretically the formation of the CPT resonance in a vapour of atoms possessing the Λ-type level structure in a gas cell of finite size. We consider both the cases of the presence and absence of the anti-relaxation coating.

2. Equations describing the CPT resonance formation

Consider a cell filled with a gas of active three-level atoms with the Λ-scheme of levels (see figure 1). We denote by $|1\rangle$ and $|2\rangle$ the two relevant sublevels of the hyperfine structure of the atomic ground state, and the excited state by $|3\rangle$.

The resonant coherent laser radiation,

$$E(\vec{r},t) = \vec{E}_1 \exp[\mathrm{i}(\vec{k}_1\vec{r} - \omega_1 t)] + \vec{E}_2 \exp[\mathrm{i}(\vec{k}_2\vec{r} - \omega_2 t)] + \text{c.c.}, \tag{1}$$

drives the optical transitions $|1\rangle \leftrightarrow |3\rangle$ and $|2\rangle \leftrightarrow |3\rangle$. The laser radiation frequencies ω_1 and ω_2 are tuned near to the resonance with the transitions $|1\rangle \leftrightarrow |3\rangle$ and $|2\rangle \leftrightarrow |3\rangle$, respectively. We denote the detunings of laser components off the corresponding transitions as Ω_1 and Ω_2, $\delta_R = \Omega_1 - \Omega_2$ is the two-photon (Raman) detuning, $\delta_L \approx \Omega_1 \approx \Omega_2$ is the single-photon (optical) detuning, γ is the decay rate of state $|3\rangle$ and Γ is the ground-state relaxation rate.

The equation describing the evolution of the atomic density matrix $\widehat{\rho}(\vec{r}, \vec{p}, t)$ in the Wigner representation reads as

$$\dot{\rho}_{ij}(\vec{r},\vec{p},t) \equiv \frac{\partial \rho_{ij}}{\partial t} + \frac{\vec{p}}{m}\nabla\rho_{ij} = -\frac{\mathrm{i}}{\hbar}\sum_k [H_{ik}\rho_{kj} - \rho_{ik}H_{kj}] + (\widehat{\widehat{\Gamma}}\widehat{\rho})_{ij}. \tag{2}$$

Here $\widehat{\widehat{\Gamma}}$ is the relaxation matrix, m is the atomic mass and $\widehat{H}$ is the Hamiltonian which can be represented as

$$\widehat{H} = \widehat{H}_0 + \hbar\widehat{V}, \tag{3}$$

with $\widehat{H}_0$ being the atomic Hamiltonian in the absence of the laser radiation, and

$$\hbar\widehat{V} = \hbar V_1 \exp[-\mathrm{i}(\omega_1 t - \vec{k}_1\vec{r})]|3\rangle\langle 1| + \hbar V_2 \exp[-\mathrm{i}(\omega_2 t - \vec{k}_2\vec{r})]|3\rangle\langle 2| + \text{h.c.} \tag{4}$$

describes the dipole interaction of the atom with the laser field (1). Here V_i is the Rabi frequency of the transition $|i\rangle \leftrightarrow |3\rangle$ ($i = 1, 2$). The phases of the resonant laser fields can be set to zero without the loss of generality, so we can consider V_i, $i = 1, 2$, as real parameters.

We assume that the translational degrees of freedom of the atoms are in equilibrium, i.e., are described by the Maxwellian distribution $M(\vec{p}) = \exp\left(-p^2/p_T^2\right)/(p_T\sqrt{\pi})^3$, where $p_T = \sqrt{2k_{\mathrm{B}}mT}$ and k_{B} is the Boltzmann constant. We adopt the following normalization condition for the density matrix:

$$\sum_i \rho_{ii}(\vec{r}, \vec{p}, t) = \frac{M(\vec{p})}{V_{\mathrm{cell}}}, \tag{5}$$

where V_{cell} is the cell volume.

In the absence of a buffer gas, and under the condition $\gamma, \gamma' \gg V_1, V_2$, where γ' is the decay rate of optical coherences and V_1, V_2 are the Rabi frequencies of the laser field components, we can adiabatically eliminate the optically excited state $|3\rangle$ and obtain the following set of equations for the ground-state density matrix:

$$\begin{aligned}
\frac{\partial f}{\partial t} + \frac{\vec{p}}{m}\nabla f &= -\left[\left(G\frac{V_1^2 + V_2^2}{\gamma'} + \Gamma\right) f - \frac{4V_1V_2}{\gamma'} F \cdot J\right] - G\frac{V_2^2 - V_1^2}{\gamma'}\frac{M(\vec{p})}{V_{\mathrm{cell}}}, \\
\frac{\partial R}{\partial t} + \frac{\vec{p}}{m}\nabla R &= -\left[G\frac{V_1^2 + V_2^2}{\gamma'} + \Gamma\right] \cdot R - \left(\delta_R - \Delta + \vec{q}\cdot\frac{\vec{p}}{m}\right) \cdot J - \frac{V_1V_2}{\gamma'} G\frac{M(\vec{p})}{V_{\mathrm{cell}}}, \\
\frac{\partial J}{\partial t} + \frac{\vec{p}}{m}\nabla J &= \left(\delta_R - \Delta + \vec{q}\cdot\frac{\vec{p}}{m}\right) \cdot R - \left[G\frac{V_1^2 + V_2^2}{\gamma'} + \Gamma\right] \cdot J - \frac{V_1V_2}{\gamma'} F \cdot f.
\end{aligned} \tag{6}$$

Here $f = f(\vec{r}, \vec{p}, t) = \rho_{22}(\vec{r}, \vec{p}, t) - \rho_{11}(\vec{r}, \vec{p}, t)$ is an inversion, $R = \mathrm{Re}\,\rho_{12}(\vec{r}, \vec{p}, t)$, $J = \mathrm{Im}\,\rho_{12}(\vec{r}, \vec{p}, t)$, $\Delta = F\left(V_1^2 - V_2^2\right)/\gamma'$, and the real coefficients G and F are defined by the following expression:

$$G + \mathrm{i}F = \frac{\gamma'}{\gamma' - \mathrm{i}(\delta_L - \vec{k}\cdot\vec{p}/m)}, \tag{7}$$

where $\vec{k} \approx \vec{k}_1 \approx \vec{k}_2$ (we consider the case of co-propagating laser modes $\vec{k}_1$, $\vec{k}_2$), $\vec{q} = \vec{k}_1 - \vec{k}_2$ ($q \ll k$). The coefficients G and F determine the efficiency of interaction of atoms with a given velocity with the laser radiation. The population of the excited state is found to be

$$\rho_{33} = \frac{G}{\gamma\gamma'}\left[V_1^2\rho_{11} + 2V_1V_2R + V_2^2\rho_{22}\right]. \tag{8}$$

In a cell without a buffer gas, γ is the spontaneous decay rate of state $|3\rangle$ and γ' is determined by the spectral width Γ_L of the laser radiation [31, 32],

$$\gamma' = \frac{\gamma + \Gamma_L}{2}. \tag{9}$$

Let us consider the processes that occur during an atom–wall collision. If a cell is coated with an anti-relaxation material, such as long-chain polymeric paraffin, atoms are not absorbed on the walls. The phase dispersion of an atom after a collision is very small. Hence, the total relaxation of the atomic momentum requires a huge number of collision events. In this case, the 'specular coherent reflection' boundary condition [22]

$$\rho_{ij}(\vec{r}, \vec{p})_{\substack{\vec{r}\in S \\ p_n>0}} = \rho_{ij}(\vec{r}, \vec{p})_{\substack{\vec{r}\in S \\ p_n<0}} \tag{10}$$

is a fair approximation.

The opposite limiting case takes place if every collision of an active atom with the cell wall results in total randomization of the atomic spin. This case can be modelled by the

'total quenching' boundary conditions [22], which assume that any coherence and population inversion are absent in the flow of atoms just reflected from the cell wall:

$$f(\vec{r},\vec{p})_{\substack{\vec{r}\in S\\ p_n>0}} = 0, \qquad \rho_{12}(\vec{r},\vec{p})_{\substack{r\in S\\ p_n>0}} = 0, \tag{11}$$

where the condition $\vec{r} \in S$ defines the coordinate points on the inner surface S of the cell and the lower index n denotes the component of the atomic momentum normal to S.

Solving equations (6) with the boundary conditions (10) or (11), using the normalization condition (5) and invoking adiabatic elimination of the excited state (equation (8)), we obtain the momentum-dependent population $\rho_{33}(\vec{r},\vec{p})$ of the excited state, which can then be averaged over the cell volume and the atomic momentum:

$$\bar{\rho}_{33} = \iint \rho_{33}(\vec{r},\vec{p})\,\mathrm{d}\vec{r}\,\mathrm{d}\vec{p}. \tag{12}$$

The power δP of the laser radiation absorbed in the cell is proportional to $\bar{\rho}_{33}$ [35]:

$$\delta P = \hbar\omega \cdot 2\gamma \cdot N \cdot \bar{\rho}_{33}, \tag{13}$$

where $\omega \approx \omega_1 \approx \omega_2$ is the optical transition frequency and N is the total number of active atoms in the cell. The CPT resonance is a narrow dip in the absorbed power spectral dependence on the two-photon detuning δ_R. Since $\delta P \propto \bar{\rho}_{33}$, we can call a CPT resonance also the corresponding minimum in the dependence $\bar{\rho}_{33} = \bar{\rho}_{33}(\delta_R)$.

3. Calculations

We now define the main parameters of the CPT resonance. The difference $\bar{\rho}_{33}^{NR} - \bar{\rho}_{33}^{R}$, where $\bar{\rho}_{33}^{NR}$ and $\bar{\rho}_{33}^{R}$ are the excited state averaged populations off the resonance and exactly at the resonance, respectively, is called the *amplitude*. The FWHM of the resonance we call the *width* and denote by Γ_{CPT}. The *contrast* is defined as

$$C(\delta_R) = \frac{\bar{\rho}_{33}^{NR} - \bar{\rho}_{33}(\delta_R)}{\bar{\rho}_{33}^{NR}}. \tag{14}$$

We consider the case $\delta_L = 0$. It follows from equation (9) that the coefficients F and G approach their maximum possible values (of the order of 1) only for atoms with momenta of the order of or less than $p_c = \gamma' m/k$. It is convenient to introduce the new parameter

$$\mu = \frac{p_c}{p_T} = \frac{\gamma' m}{k \cdot p_T} = \frac{\gamma'}{k \cdot \upsilon_T} \approx \frac{\gamma'}{\Delta_D}, \tag{15}$$

where $\upsilon_T = p_T/m$ is the thermal velocity and $\Delta_D = k\upsilon_T$ is the standard Doppler broadening.

If $\mu \ll 1$, then only sufficiently slow atoms contribute to the CPT resonance formation. Then the residual Doppler broadening of the CPT resonance is of the order of qp_c/m, i.e. much less than qp_T/m. This effect is known as laser-induced line narrowing. If $\mu \geqslant 1$, then the residual broadening of the CPT resonance is $\sim q\upsilon_T$. However, if CPT resonance is excited in a vapour cell with anti-relaxation coating, and the cell size is smaller than the half of the wavelength of the two-photon (hyperfine) transition between the levels $|1\rangle$ and $|2\rangle$, then the Dicke-type narrowing occurs [16].

In this section, we present numerical results for a CPT resonance for different values of the rate γ' of the optical relaxation and different cell lengths a. The cell radius is assumed to be much larger than the cell length, so we consider, in fact, a one-dimensional cell model. But, as was shown in [21, 33], for a coated cell these results will not be sufficiently different from the results of a three-dimensional cell.

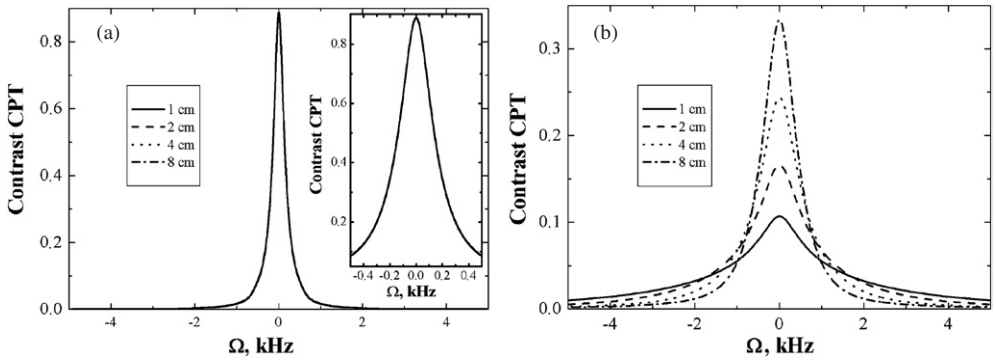

Figure 2. CPT resonance line shape for various lengths of a gas cell in the case of (a) specular-coherent reflection and (b) total quenching. $\gamma' = 2 \times 10^9\ \mathrm{s}^{-1}$, $V_1 = V_2 = 10^6\ \mathrm{s}^{-1}$, $q = 0$.

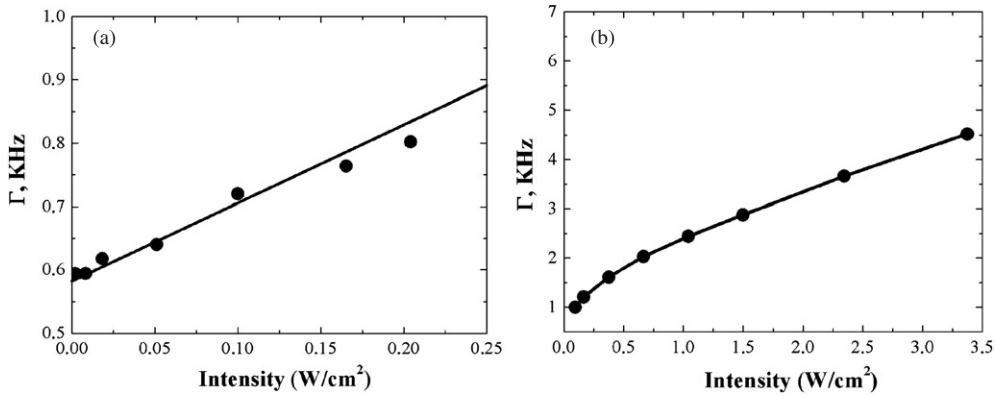

Figure 3. Dependence of CPT width on the drive-field intensities when $\gamma'\gamma \ll V_1^2 \ll \Delta_D^2\gamma'/\gamma$ (a) and at higher intensities (b).

3.1. Case of $q = 0$

Here, we consider the numerical results for a CPT resonance for different values of the rate γ' of the optical relaxation and different cell lengths a. The cell temperature is 50 °C and the relaxation rate for the ground-state manifold $\Gamma = 100\ \mathrm{s}^{-1}$. The parameters of the active atoms are chosen to be close to those of ^{87}Rb: $m = 87$ au, $\omega = kc = 2.4 \times 10^{15}\ \mathrm{s}^{-1}$, $\omega_{12} = qc \approx 0$ (i.e., $q\upsilon_T \ll \Gamma$). Such a case can be realized when the levels $|1\rangle$ and $|2\rangle$ are the Zeeman sublevels of the same hyperfine sublevels of the ground state. In this case, we could not see the Doppler broadening of the CPT resonance, and for the coated cell the CPT line shape should not depend on the cell size. But for an uncoated cell such dependence takes place because of the relaxation on the cell walls (see figure 2). We can see that the smaller the cell the lower the contrast and the broader the CPT resonance.

We also investigated the case when one component of laser field (V_1) is strong and the other (V_2) is weak in the coated cell. We found that the dependence of the CPT line width Γ_{CPT} on the strong field Rabi frequency V_1 has the linear character, $\Gamma_{\mathrm{CPT}} \approx V_1\sqrt{2\gamma'/\gamma}$, if $\gamma'\gamma \ll V_1^2 \ll \Delta_D^2\gamma'/\gamma$ (see figure 3(a)), and the quadratic character, $\Gamma_{\mathrm{CPT}} \approx V_1^2/\Delta_D$ (see figure 3(b)), at higher intensities. This result coincides with the theoretical result of [29] and experimental results of [25].

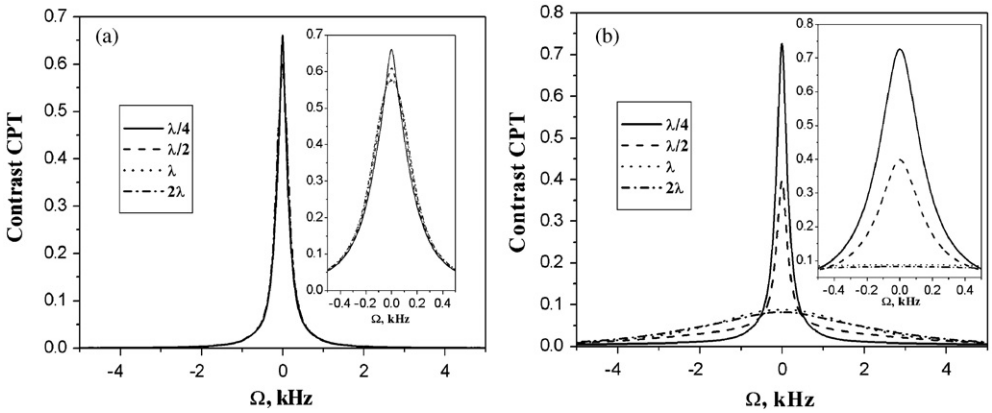

Figure 4. CPT resonance line shape for various lengths of a gas cell in the case of specular-coherent reflection conditions (a) $\gamma' = 2 \times 10^7$ s^{-1}, $V_1 = V_2 = 10^5$ s^{-1}; (b) $\gamma' = 2 \times 10^9$ s^{-1}, $V_1 = V_2 = 10^6$ s^{-1}.

3.2. Case of $q \neq 0$

The parameters of the active atoms are chosen to be close to those of ^{87}Rb: $m = 87$ au, $\omega = kc = 2.4 \times 10^{15}$ s^{-1}, $\omega_{hfs} = qc = 4.3 \times 10^{10}$ s$^{-1} = 2\pi \times 6.8$ GHz, which correspond to the $|1\rangle \leftrightarrow |2\rangle$ transition wavelength $\lambda \approx 4.4$ cm. The cell temperature is 50 °C and the relaxation rate for the ground-state manifold $\Gamma = 100$ s^{-1}. Such a choice yields $kv_T \approx 2\pi \times 315$ MHz $\approx 2 \times 10^9$ s^{-1}. $qv_T \approx 2\pi \times 5.7$ kHz $\approx 3.56 \times 10^4$ s^{-1}. According to (9), the value of γ' is determined by the laser spectral width Γ_L and not less than the half of the excited-state spontaneous decay rate, $\gamma' \geqslant \gamma/2 \approx 1.8 \times 10^7$ s^{-1}.

In figure 4, we present our results: (a) for a narrow-band laser ($\Gamma_L \ll \gamma$; $\gamma' = 2 \times 10^7$ s^{-1}, $\mu = 0.01$) and (b) for a broad-band laser ($\Gamma_L \approx 4 \times 10^9$ s$^{-1} \gg \gamma$; $\gamma' = 2 \times 10^9$ s^{-1}, $\mu = 1$), assuming the 'specular coherent reflection' boundary conditions (10). One can see from figure 4 that for $\mu = 1$ the width and the best achievable contrast of the resonance strongly depend on the cell lengths, and for $a \sim \lambda$ the widths approach the value of the residual Doppler broadening. However, for $\mu = 0.01$, there is no significant dependence of the CPT resonance parameters on the cell length. This result shows that there are two different regimes of narrowing: In the former case, the Dicke effect dominates and in the latter case LILN determines the CPT resonance properties.

Figure 5 displays the results obtained for the total quenching boundary conditions (12). In the case of light-induced narrowing (figure 5(a)) the CPT resonance weakly depends on the cell length, and the results are very similar to those presented in figure 4(a). On the other hand, the Dicke-type narrowing is quite inefficient in a cell without coating, as can be seen from figure 5(b).

Thus, we can conclude that the light-induced narrowing mechanism works independently of the size of a cell containing no buffer gas and the presence of the wall coating, in contrast to the Dicke narrowing.

3.3. Figure-of-merit for frequency standards

Comparison of efficiency of the light-induced narrowing in an uncoated cell irradiated by a laser with a narrow spectral width $\Gamma_L \ll kv_T$ and in a coated cell irradiated by a broad-band laser is of great practical interest. It is known [35] that the figure-of-merit of a CPT-based

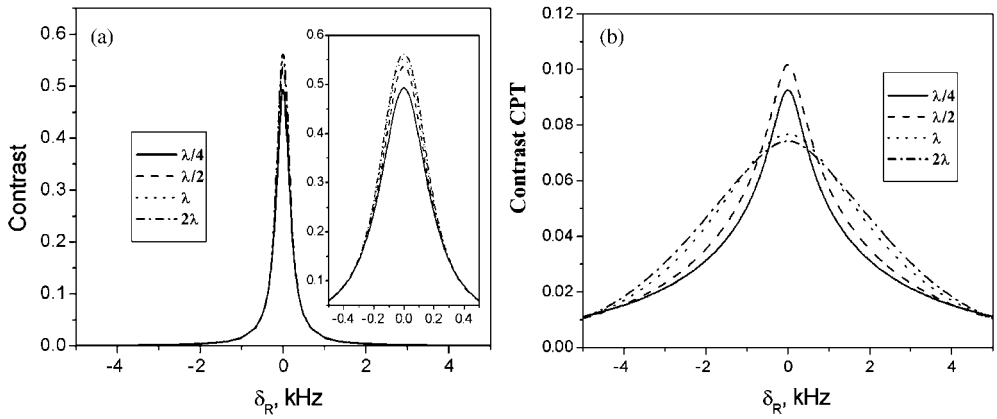

Figure 5. CPT resonance line shape for various lengths of a gas cell in the case of total quenching conditions (a) $\gamma' = 2 \times 10^7\ \mathrm{s}^{-1}$, $V_1 = V_2 = 10^5\ \mathrm{s}^{-1}$; (b) $\gamma' = 2 \times 10^9\ \mathrm{s}^{-1}$, $V_1 = V_2 = 10^6\ \mathrm{s}^{-1}$.

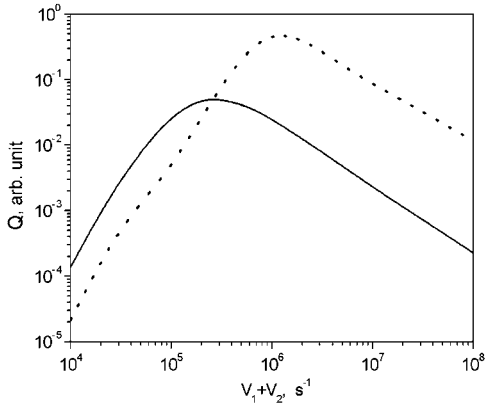

Figure 6. Parameter Q versus the Rabi frequency of laser fields. The gas cell length $a = \lambda/4$. The solid curve corresponds the total quenching boundary conditions with $\gamma' = 2 \times 10^7\ \mathrm{s}^{-1}$, and the dotted curve corresponds the specular-coherent boundary conditions with $\gamma' = 2 \times 10^9\ \mathrm{s}^{-1}$.

quantum discriminator that determines the stability of the frequency standard is proportional to the product of the second derivative of the absorbed power over the two-photon detuning and the width of the linear part of the discrimination curve, and is inversely proportional to the square root of the intensity of the radiation approaching the photodetector. Since, according to equation (15), the absorbed power is linear in $\bar{\rho}_{33}$, and the intensity of the ith component is quadratic in the corresponding Rabi frequency a V_i, the figure-of-merit for the CPT resonance can be estimated by means of the quantity

$$Q = \frac{s\Gamma_s}{V_1 + V_2}, \tag{16}$$

where $s = \left|d^2\bar{\rho}_{33}(\delta_R)\big/d\delta_R^2\right|$ at the absorption minimum and Γ_s is the width of the linear part of the discrimination curve.

We show in figure 6, the results of the calculation of the parameter Q for $\mu = 0.01$ and the boundary conditions (12), and $\mu = 1$ and the boundary conditions (11). We assume that

the cell length is $a = \lambda/4$ and the Rabi frequencies of the two transitions are equal, $V_1 = V_2$. The best value of Q in the Dicke narrowing regime ($\mu = 1$) is greater by approximately an order of magnitude than in the LILN regime ($\mu = 0.01$). The explanation is that in the LILN regime the number of atoms contributing to the CPT resonance formation is sufficiently less than that in the Dicke narrowing regime.

4. Conclusions

In the present paper, we have investigated theoretically the formation of the CPT resonance in a finite-size cell with and without an anti-relaxation coating. The existence of two distinct regimes of narrowing (light-induced and Dicke-type) has been demonstrated. The light-induced narrowing mechanism is effective only in the case of excitation by a narrow-band laser ($\Gamma_L \ll k\upsilon_T$), and the narrowing weakly depends on the cell size and the coating type. On the other hand, the use of broad-bandwidth laser radiation and coated cells allows us to improve the stability of the frequency standard by an order of magnitude.

Acknowledgments

The work is supported by the INTAS-CNES grant 06-1000024-9321 and the Fund for Non-Profit Programs 'Dinastiya'.

References

[1] Leibfried D, Blatt R, Monroe C and Wineland D 2003 *Rev. Mod. Phys.* **75** 281
[2] Lukin M D 2003 *Rev. Mod. Phys.* **75** 457
[3] Fleischhauer M, Imamoglu A and Marangos J P 2005 *Rev. Mod. Phys.* **77** 633
[4] Klein M, Novikova I, Phillips DF and Walsworth R L 2006 *J. Mod. Opt.* **53** 2583
[5] Kitching J, Knappe S and Hollberg L 2002 *Appl. Phys. Lett.* **81** 553
[6] Knappe S, Shah V, Peter D, Schwindt D, Hollberg L, Kitching J, Liew L and Moreland J 2004 *Appl. Phys. Lett.* **85** 1460
[7] Vanier J, Levine W, Janssen P and Delaney M J 2003 *IEEE Trans. Instrum. Meas.* **52** 258
[8] Peter D, Schwindt D, Knappe S, Shah V, Hollberg L, Kitching J, Liew L and Moreland J 2004 *Appl. Phys. Lett.* **85** 6409
[9] Yashuk V V, Granwehr J, Kimbal D F l, Rochester S M, Trabesinger A H, Urban J T, Budker D and Pines A 2004 *Phys. Rev. Lett.* **93** 160801
[10] Stahler M *et al* 2002 *Opt. Lett.* **27** 1472
[11] Akulshin A, Celikov A and Velichansky V 1991 *Opt. Commun.* **84** 139
[12] Aspect A *et al* 1988 *Phys. Rev. Lett.* **61** 826
[13] Agap'ev B D, Gornyi M B, Matisov B G and Rozhdestvenskii Yu V 1993 Coherent population trapping in quantum systems *Phys.—Usp.* **36** 763
[14] Vanier J 2005 *Appl. Phys.* B **81** 421
[15] Vanier J and Audoin C 1989 *The Quantum Physics of Atomic Frequency Standards* (Bristol: Adam Hilger) p 1567
[16] Dicke R H 1953 *Phys. Rev.* **89** 472
[17] Brandt S, Nagel A, Wynands R and Meschede D 1997 *Phys. Rev.* A **56** 2
[18] Robinson H, Ensberg E and Dehmel H 1958 *Bull. Am. Phys. Soc.* **3** 9
[19] Graf M T, Kimball D F, Rochester S M, Kerner K, Wong C, Budker D, Alexandrov E B, Balabas M V and Yashchuk V V 2005 *Phys. Rev.* A **72** 023401
[20] Robinson HG and Johnson C E 1982 *Appl. Phys. Lett.* **40** 771
[21] Frueholz RP and Volk C H 1985 *J. Phys. B: At. Mol. Phys.* **18** 4055
[22] Agap'ev B D, Gornyi M B and Matisov B G 1988 *J. Tekh. Fiz.* **58** 2286
[23] Budker D, Hollberg L, Kimball D F, Kitching J, Pustelny S and Yashchuk V V 2005 *Phys. Rev.* A **71** 012903
[24] Guzman J S, Wojciechowski A, Stalnaker J E, Tsigutkin K, Yashchuk V V and Budker D 2006 *Phys. Rev* A **74** 053415

[25] Ye CY and Zibrov A S 2002 *Phys. Rev.* A **65** 023806
[26] Alzetta G, Gozzini S, Lucchesini A, Cartaleva S, Karaulanov T, Marinelli C and Moi L 2004 *Phys. Rev.* A **69** 063815
[27] Feld MS and Javan A 1969 *Phys. Rev.* **2** 177
[28] Taichenachev A F, Tumaikin AM and Yudin V I 2000 *JETP Lett.* **72** 173
[29] Javan A, Kocharovskaya O, Lee H and Scully M O 2002 *Phys. Rev.* A **66** 013805
[30] Lee H, Rostovtsev Yu, Bednar C J and Javan A 2003 *Appl. Phys. B: Laser Opt.* **76** 33
[31] Kazakov G A, Matisov B G, Mazets I E and Rozhdestyenskii Yu V 2006 *J. Tekh. Fiz.* **76** 20
[32] Mazets I E and Matisov B G 1992 *JETP* **101** 26
[33] Agap'ev B D, Gornyi M B and Matisov B G 1987 *JETP* **92** 1995
[34] Agap'ev B D, Gornyi M B and Matisov B G 1989 *JETP* **95** 81
[35] Gornyi M B *et al* 1987 *Zh. Tekh Fiz.* **57** 740